Axial dispersion in liquid flow through packed reticulated metallic foams and fixed beds of different structures

Agnès Montillet, J. Comiti, J. Legrand

The Chemical Engineering Journal, 52 (1993) 63–71

Axial dispersion in liquid flow through packed reticulated metallic foams and fixed beds of different structures

A. Montillet, J. Comiti and J. Legrand

Laboratoire de Génie de Procédés, Institut Universitaire de Technologie, BP 420, F-44606 Saint Nazaire Cédex (France)

(Received March 20, 1992)

Abstract

This paper deals with the experimental study of the axial dispersion phenomenon during flow through and by fixed beds packed with sheets of nickel foams. Its purpose is to characterize the hydrodynamic behaviour of a liquid flowing through different nickel foams according to configurations corresponding to the two working modes of volumic electrodes. A comparison of axial dispersion in liquid flow through various porous media determined by using the same procedure is presented. The axial dispersion is very low for flow through reticulated nickel foams, while tightly packed beds of very anisotropic flat plates show a very dispersive behaviour. For all other media a single correlation equation based on dimensionless numbers taking structural parameters into account is proposed.

1. Introduction

Metallic foams are highly porous materials with a typical reticulated structure organized in alveoli open to each other. Therefore such material is characterized by an important specific surface area and a large permeability [1]. It appears to be a potentially interesting medium for electrochemical engineering applications such as development of very compact volumic electrodes [2].

In the first part of this paper we focus on the hydrodynamical behaviour of a liquid flowing through different nickel foams. Since this material is supplied in the form of thin sheets, two configurations were tested:

(1) the flow-through configuration where the mean direction of the flow is perpendicular to the plane of the sheets;

(2) the flow-by configuration where the mean direction of the flow is parallel to the plane of the sheets.

These two configurations correspond to the two working modes of porous volumic electrodes in which the flow direction and the current lines are either parallel (flow-through configuration) or perpendicular (flow-by configuration).

The aim of the second part of the paper is to compare the axial dispersion for liquid flow through various porous media: highly porous reticulated nickel foams, fixed beds of isotropic particles (spheres) and of parallelepipedal and cylindrical anisotropic particles, and packed beds of Raschig rings.

For our purpose the experimental results are presented using two categories of dimensionless numbers: the first corresponds to a classical representation, namely reactor Peclet number *vs.* superficial Reynolds number, and the second uses Peclet and Reynolds numbers defined by the structural properties of the studied porous media.

2. Experimental determination of liquid flow behaviour through nickel foams

The flow through a packed bed is often described by the dispersed plug flow model; the main parameter of this model is the axial dispersion coefficient D_{ax}. The radial dispersion can generally be neglected in comparison with axial dispersion. The basic differential equation giving the instantaneous local tracer concentration $C=C(z, t)$ after a uniform injection of this tracer over the cross-section of a packed bed is

$$\frac{\partial C}{\partial t} = D_{ax} \frac{\partial^2 C}{\partial^2 z} - \frac{U_o}{\epsilon} \frac{\partial C}{\partial z} \quad (1)$$

where z is the axial coordinate along the general flow direction, U_o is the mean superficial fluid velocity and ϵ is the mean bed voidage.

0923-0467/93/$6.00

Most experimental works concern the determination of the axial dispersion coefficient in flow through packed beds of particles; only a few studies deal with hydrodynamic dispersion in flow through either natural [3, 4] or sintered [5] consolidated media. However, D_{ax} values seem to be lacking for the case of liquid flow through highly porous reticulated media such as metallic or polyurethane foams. Bacri *et al.* [4] have studied the flow through a foam-like fireproof brick with a porosity value of 0.655. In the present work the case of flow through nickel foams is examined.

2.1. Experimental procedure

2.1.1. Nickel foams

Three grades of nickel foams, namely G45, G60 and G100, are studied. Like those made of polyurethane, metallic foams are characterized by their manufacturer according to their grade values, *i.e.* the number of pores present in the structure per inch. The porosities of the considered grades range from 0.973 to 0.978. The nickel foams used in this work are supplied in the form of thin sheets (thickness about 2.5 mm).

The particular structure of metallic foams is a reticulated one: a representative element cell of this porous medium can be schematized by a spherical alveolus largely open to the neighbouring alveoli. Owing to this structure, porosities close to unity and high specific surface areas are concomitantly available. The nickel foams used in this work were purchased from Sorapec [6]; previous studies devoted to the determination of their specific surface areas by various methods are detailed in refs. 1 and 7. The values of the specific surface area of nickel foams G45 and G60 offered to fluid flow are given in Table 2 (see Section 3); they are obtained by the analysis of pressure drop measurements using a suitable flow model [1].

2.1.2. Apparatus and methodology

The flow behaviour through nickel foams has been characterized by means of the experimental determination of the residence time distribution (RTD) using a polarographic method. This technique was previously used by Fleischmann *et al.* [8] for studying the pump cell and by Barthole [9] for the determination of liquid hold-up in fixed beds with gas–liquid flow.

The principles of the experimental and calculation methods used for the determination of the axial dispersion coefficient were previously described in refs. 10 and 11. A schematic diagram of the experimental method in the flow-through configuration is shown in Fig. 1.

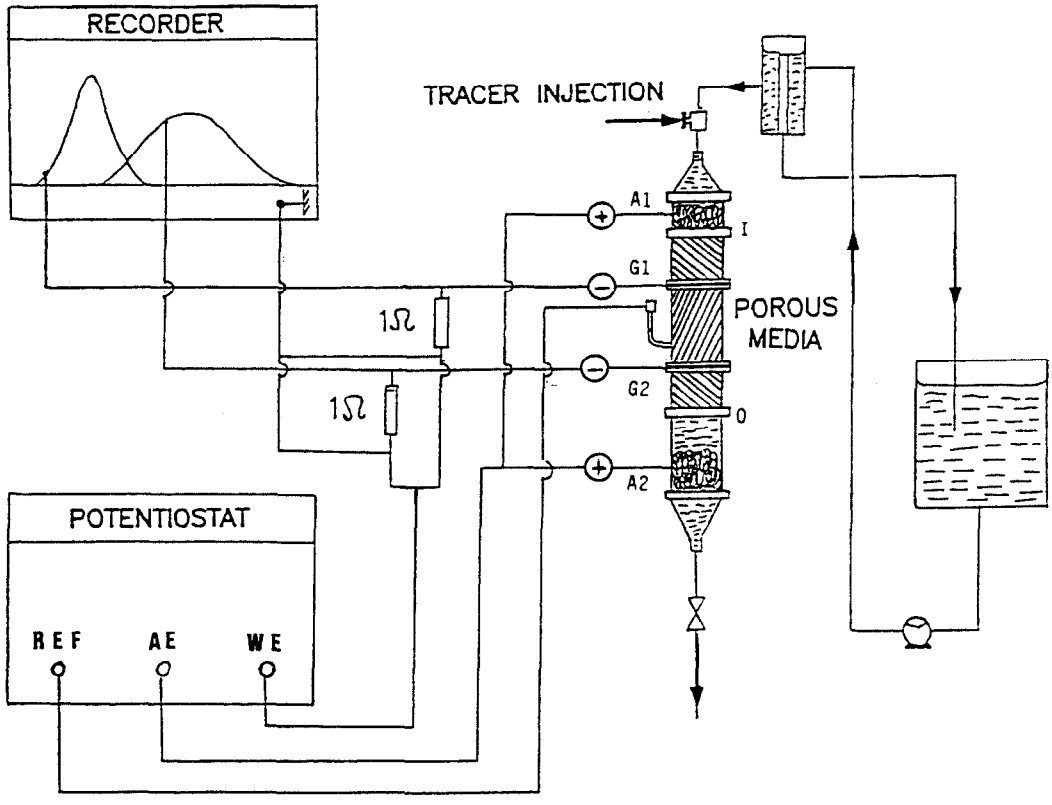

Fig. 1. Schematic diagram of experimental apparatus in flow-through configuration.

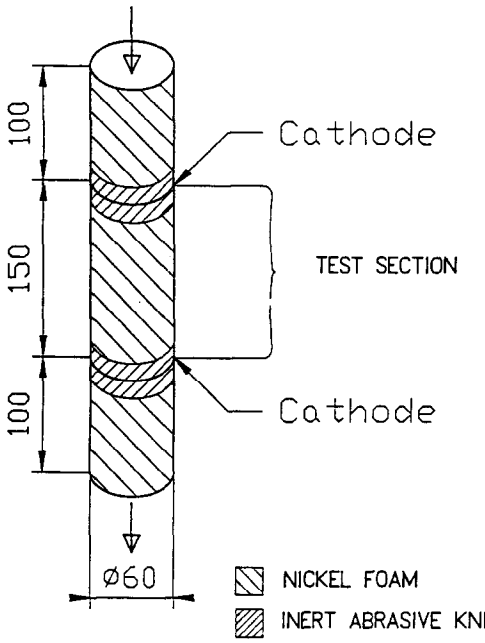

Fig. 2. Cylindrical cell packed with disks of nickel foam, flow-through configuration.

In the experiments in this work the flowing liquid is an aqueous electrolyte containing 0.5 mol l^{-1} NaOH, 2×10^{-3} mol l^{-1} $K_3Fe(CN)_6$ and 5×10^{-2} mol l^{-1} $K_4Fe(CN)_6$ maintained at 30 ± 0.2 °C. At this temperature the liquid density ρ is 1027 kg m^{-3} and its dynamic viscosity μ is 0.897×10^{-3} Pa s.

A cylindrical cell packed with disks of nickel foam has been used in order to study the flow-through configuration (Fig. 2) and a parallelepipedal cell filled with rectangular sheets of foam has been used for the flow-by configuration (Fig. 3). In each configuration three parts have to be distinguished: an upstream calming section I–G1, a test section located between the two nickel grids G1 and G2 working as cathodic sensors, and a downstream calming section G2–O. An electrically inert material consisting of a thin piece of abrasive knit separated the nickel foams from the cathodic grids. In the flow-through configuration the anode consists of two nickel wire knits of large surface area located at the entrance and bottom of the cell. In the flow-by configuration the two calming sections I–G1 and G2–O served as the anode. The reference electrode is a platinum electrode located between G1 and G2.

The electrodes are cleaned with a 0.5 mol l^{-1} solution of sulphuric acid. The nickel grids, acting as the cathode, are activated *in situ* by cathodic reduction with a 0.5 mol l^{-1} solution of sodium hydroxide. Oxygen background currents are avoided by a final bubbling of the solution with nitrogen.

All experiments have been performed under limiting current conditions at the cathodic grids where the electrochemical reduction of ferricyanide ions occurs. A small volume of saturated aqueous potassium ferricyanide solution was injected before the cell entrance and the resulting limiting current intensity, $I_1(t)$ and $I_2(t)$ on the two cathodic sensors G1 and G2 respectively, was registered as a function of time. For given hydrodynamic conditions in the cell the mean mass transfer coefficient k between the electrolyte and each cathode is constant; therefore the limiting diffusion current intensity I at a grid was directly proportional to the ferricyanide concentration C.

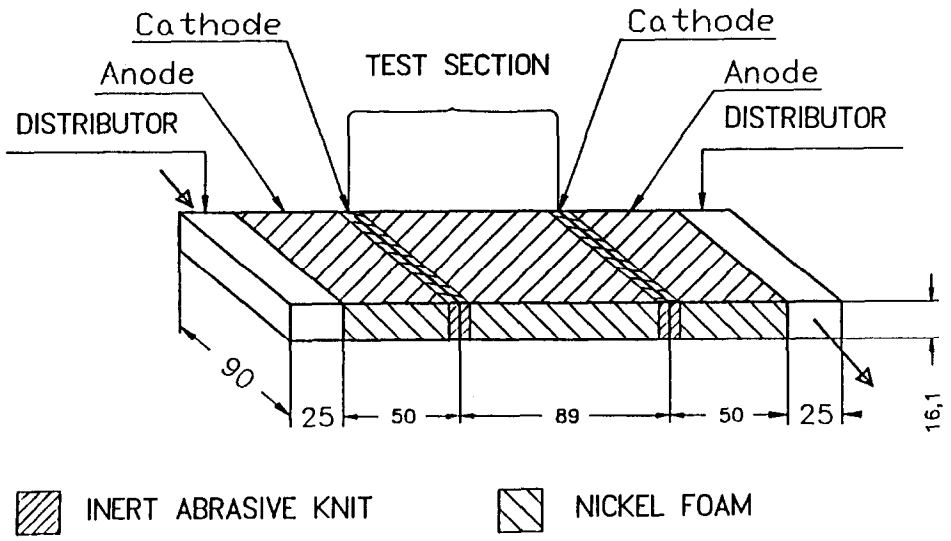

Fig. 3. Parallelepipedal cell packed with rectangular sheets of foam, flow-by configuration.

Analysis of the experimental signals $I_1(t)$ and $I_2(t)$ allowed the determination of the mean residence time and the axial dispersion coefficient. The calculation method, based on curve fitting in the time domain [12], is detailed in refs. 10 and 11.

2.2. Results

For each grade and each configuration the axial dispersion coefficient D_{ax} is a linear function of the superficial velocity U_o:

$$D_{ax} = \alpha U_o \quad (2)$$

The obtained values of α are given in Table 1 and the experimental results are shown in Fig. 4.

For the two grades tested in each flow configuration, G45 and G60 respectively, the ratio of α coefficients measured in flow-through and flow-by configurations is close to unity.

TABLE 1. Values of α

Foam grade	Configuration			
	Flow-through		Flow-by	
	U_o (m s^{-1})	$10^3\alpha$ (m)	U_o (m s^{-1})	$10^3\alpha$ (m)
G45	0.0011–0.0028	1.26±0.18	0.002–0.004	1.09±0.14
G60	0.0007–0.0088	1.01±0.14	0.0007–0.0088	0.90±0.15
G100	Not studied		0.002–0.006	1.30±0.14

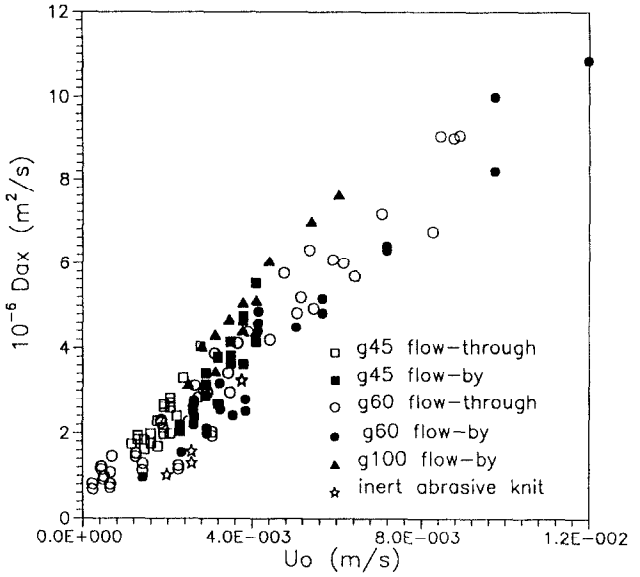

Fig. 4. Experimental axial dispersion coefficient *vs.* superficial velocity.

Because of the geometrical characteristics of the cells, wall effects can be neglected. Thus the axial dispersion phenomenon observed in each configuration may be considered to be representative of the structure of the nickel foams. Since their structure is quasi-isotropic in the three directions of space [1, 13] it is logical to obtain nearly identical values of α in the two studied configurations.

The behaviour of the liquid flow through the electrically inert separator between the metallic foams and cathodes has also been studied. One can observe in Fig. 4 that the corresponding values of D_{ax} as a function of U_o are close to those obtained for the foams. Moreover, the volume filled with the abrasive knit is 6.6% of the total volume of the test section in the flow-through configuration and 11.2% in the flow-by configuration; thus the influence of the abrasive knit on the experimental value of D_{ax} for the nickel foams may be considered negligible.

3. Dimensionless correlations – comparison between various porous media

Examination of the experimental studies of axial dispersion for flow through porous media performed during the last three decades shows that the results are significantly scattered [14]. The results may depend on experimental conditions, on the nature of the tracer injection and detection and on the method of calculation of axial dispersion coefficients. In order to obtain a more accurate comparison between various porous media, the experiments were performed using the same experimental method and apparatus and the same method of calculation. The collected data concern flow through fixed beds packed with glass spheres [15], long cylinders [16], square-based parallelepipedal particles of different height-to-side ratios (e/a) [10, 11], Raschig rings and nickel foams previously described in this paper. The studied fixed beds were packed with identical particles, the geometrical characteristics of which are given in Table 2 together with the bed voidage and the ratio of the length of the bed to the larger dimension of the particle.

The studied porous media have very different structures and are characterized by a very large range of porosity (0.36–0.98). One can distinguish:

(1) fixed beds of spheres – isotropic medium;

(2) beds tightly packed with anisotropic convex particles – long cylinders, flat plates constituting a stratified medium;

(3) fixed beds of Raschig rings;

(4) metallic foams – reticulated medium.

TABLE 2. Geometrical characteristics of particles and packed beds (ϕ column is the diameter of the cylindrical cell; d_{min} and d_{max} are the higher and lower dimensions of the particle respectively)

Porous medium	Geometric dimensions	$\frac{\phi \text{ column}}{d_{max}}$	$\frac{d_{min}}{d_{max}}$	Bed void fraction	A_{vd} (m^{-1})	τ
Spheres	Diameter 2×10^{-3} m	30	1	0.36	3080	1.44
	Diameter 3×10^{-3} m	20	1	0.36	2060	1.44
	Diameter 4×10^{-3} m	15	1	0.36	1520	1.44
	Diameter 5×10^{-3} m	12	1	0.36	1210	1.44
Cylinders	Diameter 1.00×10^{-3} m Length 5.49×10^{-3} m	10.7	0.18	0.39	3490	1.90
Flat plates (thickness e, side a)	$e=0.517\times10^{-3}$ m $a=5.05\times10^{-3}$ m $e/a=0.102$	8.4	0.07	0.46	2320	3.49
	$e=1.045\times10^{-3}$ m $a=5.00\times10^{-3}$ m $e/a=0.209$	8.4	0.15	0.35	1440	2.77
	$e=2.180\times10^{-3}$ m $a=4.96\times10^{-3}$ m $e/a=0.440$	8.2	0.30	0.31	1160	2.01
Raschig rings	Length 7×10^{-3} m Diameter 7×10^{-3} m	6.1	0.71	0.58	–	–
Nickel foam G60	60 pores per inch Mean pore diameter 6.1×10^{-4} m	–	–	0.975	2550×10^{2}	1.17
Nickel foam G45	45 pores per inch Mean pore diameter 9.6×10^{-4} m	–	–	0.978	1860×10^{2}	1.24

The particle-packed beds are characterized by a low specific surface area offered to fluid flow ($1000 < A_{vd} < 3500\ m^{-1}$). In contrast, the reticulated media consisting of nickel foams G45 and G60 have a specific surface area greater than 190 000 m^{-1}.

The experimental results, obtained for all these porous media under the experimental conditions corresponding to the study in the flow-through configuration (Figs. 1 and 2) as D_{ax} *vs.* U_o, are given in Table 3 and Fig. 5.

We present and compare the results by using two different types of correlations.

(1) First, we propose correlation equations between the Peclet number Pe_l and the superficial Reynolds number Re_o (Fig. 6, Table 3). Pe_l is the Peclet number Pe_L related to a reactor length L equal to 1 m:

$$Pe_L = \frac{U_o L}{D_{ax}\epsilon} \qquad (3)$$

$$Pe_l = Pe_L \quad \text{for } L = 1 \text{ m}$$

Indeed, most of the porous media considered in this study may be used in chemical reactors: cylindrical and spherical particles in catalytic fixed bed reactors; metallic foams and spherical particles in electrochemical reactors; Raschig rings in absorbers; parallelepipedal particles simulate wood chips reacting in digesters of the paper pulp industry. The value of Pe_L directly influences the mass balance of such reactors and it is a useful quantitative parameter for evaluating the scatter between the plug flow ideal behaviour and that of the real reactor.

From Fig. 6 one can note particular behaviours of the flow through two kinds of media.

(a) The axial dispersion is very low for flow through reticulated foams ($Pe_l \approx 1000$).

(b) In contrast, the value of Pe_l is clearly the lowest and the axial dispersion the highest for beds tightly packed with anisotropic flat plates (square-based parallelepipedal particles of ratio $e/a = 0.1$). We have found $27 < Pe_l < 57$ for $1.6 < Re_o < 350$. The values of Pe_l for all other packings are intermediate: $100 < Pe_l < 380$ for $1.7 < Re_o < 2220$.

(2) Secondly, we propose to take into account the structure of the porous media by using the capillary-type model presented by Comiti and Renaud [17].

The porous medium is represented by a bundle of cylindrical tortuous pores of diameter d_p and

TABLE 3. Experimental correlations obtained with various packed beds

Bed	U_o (m s^{-1})	Correlation $D_{ax}=f(U_o)$ (m^2 s^{-1})	Re_o	Correlation $Pe_l=f(Re_o)$	Re_{pore}	Correlation $Pe_{pore}=f(Re_{pore})$
Spheres, 2 mm	1.8×10^{-4}–3.8×10^{-2}	$7.6\times10^{-3}U_o$	10.5–2220	365	0.229–110	0.394
Spheres, 3 mm	5.1×10^{-5}–8.5–10^{-3}	$11.4\times10^{-3}U_o$	3.0–497	243		
Spheres, 4 mm	7.0×10^{-5}–1.1×10^{-2}	$15.2\times10^{-3}U_o$	4.1–877	183		
Spheres, 5 mm	7.0×10^{-5}–1.5×10^{-2}	$19.0\times10^{-3}U_o$	4.1–641	146		
Cylinders	4.0×10^{-5}–1.1×10^{-2}	$1.25\times10^{-2}U_o^{1.06}$	1.7–640	$396Re_o^{-0.06}$	0.104–38.1	$0.466Re_{pore}^{-0.06}$
Flat plates, $e/a=0.102$	2.7×10^{-5}–0.6×10^{-2}	$1.87\times10^{-2}U_o^{0.86}$	1.6–350	$25Rc_o^{0.14}$	0.292–65.0	$0.162Rc_{pore}^{0.14}$
Flat plates, $e/a=0.209$	6.4×10^{-5}–0.6×10^{-2}	$8.53\times10^{-3}U_o^{0.88}$	2.7–350	$89Re_o^{0.12}$	0.737–71.5	$0.451Re_{pore}^{0.12}$
Flat plates $e/a=0.440$	4.6×10^{-5}–0.6×10^{-2}	$1.43\times10^{-2}U_o^{0.90}$	2.7–350	$94Re_o^{0.08}$	0.449–59.5	$0.339Re_{pore}^{0.08}$
Raschig rings	7.6×10^{-5}–3.7×10^{-3}	$1.69\times10^{-2}U_o$	5.2–254	102	–	–
Foam G60	2.4×10^{-4}–8.9–10^{-3}	$1.01\times10^{-3}U_o$	16.5–611	1025	0.20–7.5	0.737
Foam G45	1.1×10^{-3}–2.8×10^{-3}	$1.26\times10^{-3}U_o$	75.5–192	811	1.53–3.9	0.776

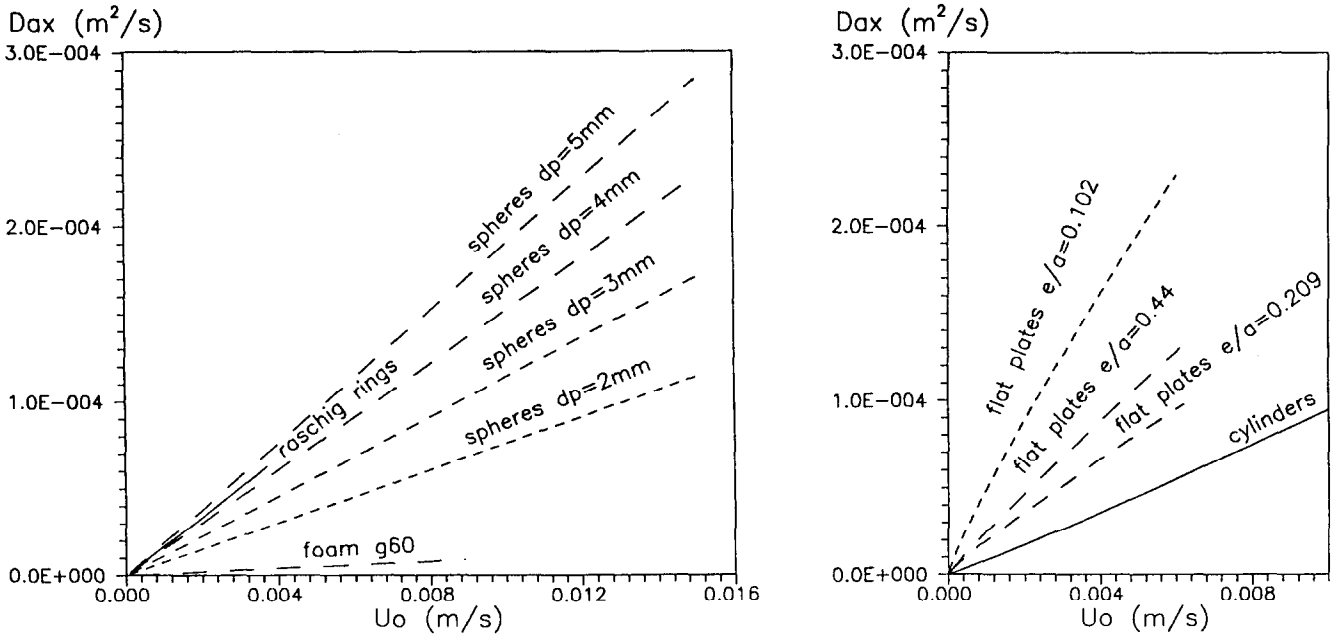

Fig. 5. Comparison of D_{ax} *vs.* U_o for various packed beds (correlation equations).

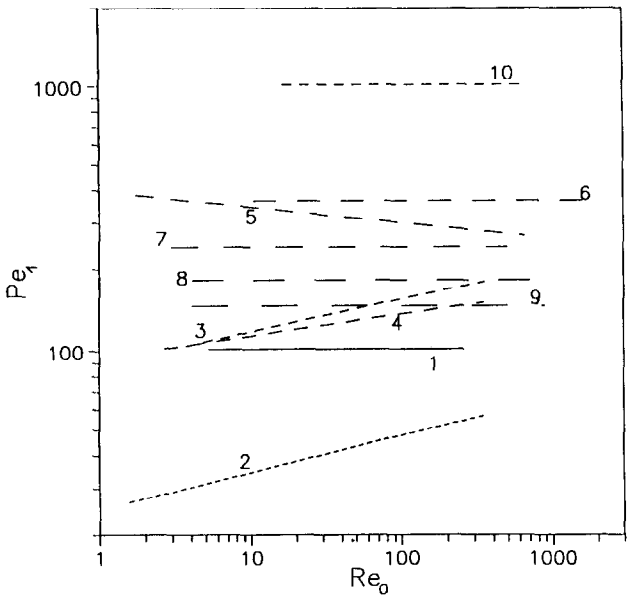

Fig. 6. Comparison of Pe_1 *vs.* Re_o for various packed beds (correlation equations: 1, Raschig rings; 2, flat plates, $e/a=0.102$; 3, flat plates, $e/a=0.209$; 4, flat plates, $e/a=0.440$; 5, cylinders; 6, spheres, 2 mm; 7, spheres, 3 mm; 8, spheres, 4 mm; 9, spheres, 5 mm; 10, foam G60).

length l. If H is the height of the fixed bed, the tortuosity is defined as

$$\tau = \frac{l}{H} \tag{4}$$

The diameter of the pores is

$$d_p = \frac{4\epsilon}{A_{vd}(1-\epsilon)} \tag{5}$$

where A_{vd} is the dynamic specific surface area defined by

$$A_{vd} = \frac{\text{real surface area presented to the flow}}{\text{volume of solid}} \tag{6}$$

The mean velocity in the pore may be calculated as

$$U = U_o \frac{\tau}{\epsilon} \tag{7}$$

Let us define a Reynolds number based on the mean pore diameter d_p and the mean velocity U in the pore:

$$Re_{pore} = \rho \frac{U_o \tau}{\epsilon} \frac{d_p}{\mu} \tag{8}$$

Generally, the correlations concerning axial dispersion in fixed beds are presented using a dimensionless Peclet number based on the particle diameter and the interstitial velocity:

$$Pe_i = \frac{U_o d_{particle}}{\epsilon D_{ax}} \tag{9}$$

One can point out that the definition of a particle diameter, which is arbitrary for non-spherical particles, has no physical meaning for a reticulated medium. Moreover, in our opinion, the structure of the bed influences the value of the axial dispersion

coefficient. Therefore we propose to define a new dimensionless criterion based on the mean pore diameter d_p and the mean pore velocity U in order to correlate experimental results corresponding to various porous media of different structures:

$$Pe_{pore} = \frac{Ud_p}{D_{ax}} = \frac{4U_o}{\tau(1-\epsilon)A_{vd}D_{ax}} \quad (10)$$

For all the studied porous media of very different structures, correlation equations giving Pe_{pore} as a function of Re_{pore} have been calculated. The structural parameters τ and A_{vd} have been previously obtained by pressure drop measurements for newtonian liquid flow [1, 16, 17]. The correlation equations are given in Table 3; experimental data are plotted as Pe_{pore} *vs.* Re_{pore} in Fig. 7.

The values of Pe_{pore} in the range $0.1 < Re_{pore} < 100$ for fixed beds of long cylinders, spheres of different diameters and square-based parallelepipedal particles of height-to-side ratio $e/a = 0.44$ are relatively close. For all these experimental points one can propose a single correlation

$$Pe_{pore} = 0.43 \pm 0.10 \quad (11)$$

In contrast, the values for beds of metallic foams and tightly packed beds of very flat parallelepipedal particles are significantly different: the corresponding mean values of Pe_{pore} are 0.2 for flat plates and 0.74 and 0.96 for metallic foams G60 and G45 respectively.

Taking into account the tortuosity and dynamic surface area of these porous media is not sufficient to obtain a universal correlation equation including these media characterized by a very particular structure. However, the range of variation in Pe_{pore} for all the experiments on the beds packed with particles is clearly lower than the range of variation in the Peclet number Pe_i based on particle diameter classically used in the literature.

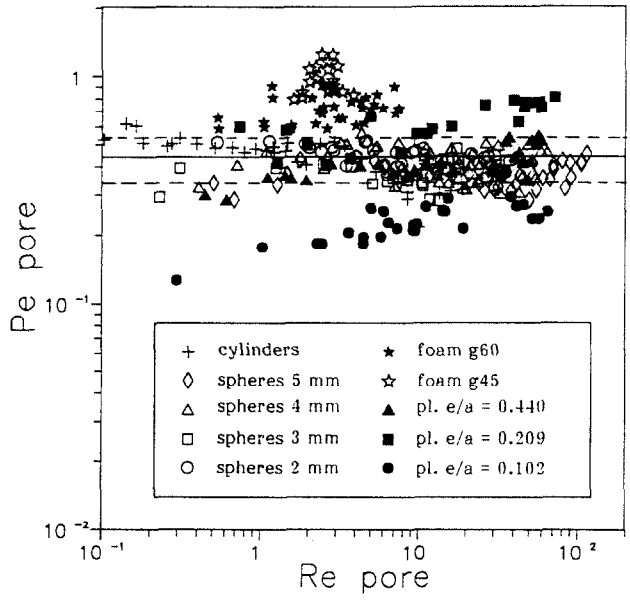

Fig. 7. Comparison of experimental data for various packed beds in terms of Pe_{pore} *vs.* Re_{pore} (——, $Pe_{pore} = 0.43 \pm 0.1$).

4. Conclusions

The axial dispersion phenomenon in liquid flow through metallic foams is very limited and nearly identical in flow-through and flow-by configurations.

A comparison of axial dispersion in liquid flow through various porous media, determined by using the same procedure, has been performed.

A first type of correlation expressing the Peclet number based on a unit length of reactor as a function of the superficial Reynolds numbers is proposed. Its main interest is to quantify the influence of axial dispersion on the conversion performance in fixed bed reactors.

Subsequently, a dimensionless presentation of the results taking into account the structural properties of the porous media has been proposed. It allows us to obtain a single correlation for a large number of porous media. However, this correlation does not represent the behaviour of flow through porous media of a very particular structure, such as metallic foams of very low tortuosity and very high bed void fraction or tightly packed beds of very anisotropic flat plates which present a high tortuosity value ($\tau = 3.5$) inducing a large axial dispersion. Bearing these exceptions in mind, eqn. (11) may be used for engineering purposes in order to evaluate axial dispersion coefficients for liquid flow through most porous media.

References

1 A. Montillet, J. Comiti and J. Legrand, *J. Mater. Sci.*, *27* (1992) 4460.
2 S. Langlois and F. Coeuret, *J. Appl. Electrochem.*, *19* (1989) 51.
3 D.L. Kinzel and G.A. Hill, *Can. J. Chem. Eng.*, *67* (1989) 39.
4 J.C. Bacri, N. Rakotomalala and D. Salin, *Phys. Rev. Lett.*, *58* (1987) 2035.
5 E. Charlaix, J.P. Hulin and T.J. Plona, *Phys. Fluids*, *30* (1987) 1690.
6 Sorapec, 192 Rue Carnot, F-94120 Fontenay sous Bois, France.
7 S. Langlois and F. Coeuret, *J. Appl. Electrochem.*, *19* (1989) 43.

8 M. Fleischmann, J. Ghoroghchian and R.E.W. Jansson, *J. Appl. Electrochem.*, *9* (1979) 437.
9 G. Barthole, *Thesis Dr.Ing.*, Institut National Polytechnique de Lorraine, Nancy, 1983.
10 J. Comiti, *Thesis*, Institut National Polytechnique, Grenoble, 1987.
11 P. Legentilhomme, J. Legrand and J. Comiti, *J. Appl. Electrochem.*, *19* (1989) 263.
12 N. Wakao and S. Kaguei, *Heat and Mass Transfer in Packed Beds*, Gordon and Breach, London, 1982.
13 A.T. Huber and L.J. Gibson, *J. Mater. Sci.*, *23* (1988) 3031.
14 C.Y. Wen and L.T. Fan, *Models for Flow Systems and Chemical Reactors*, Dekker, New York, 1975.
15 M. Hilal and J. Comiti, *Récents Prog. Génie Procédés, Lavoisier*, *3* (1989) 451.
16 D. Brunjail and J. Comiti, *Chem. Eng. J.*, *45* (1990) 123.
17 J. Comiti and M. Renaud, *Chem. Eng. Sci.*, *44* (1989) 1539.

Appendix A: Nomenclature

a	side of square-based parallelepipedal particles (m)
A_{vd}	dynamic specific surface area (m^{-1})
C	ferricyanide concentration (mol m^{-3})
d_p	mean equivalent pore diameter (m)
$d_{particle}$	particle diameter (m)
D	diameter of cylindrical cell (m)
D_{ax}	axial dispersion coefficient (m^2 s^{-1})
e	thickness of parallelepipedal particles (m)
H	active bed height (m)
I	limiting diffusion current intensity (A)
$I_1(t)$	limiting diffusion current intensity at cathodic sensor G1 (A)
$I_2(t)$	limiting diffusion current intensity at cathodic sensor G2 (A)
k	mean mass transfer coefficient (m s^{-1})
l	length of cylindrical tortuous pores (m)
L	length of reactor (m)
Pe_i	interstitial Peclet number, $U_o d_{particle} \epsilon^{-1} D_{ax}^{-1}$
Pe_L	Peclet number related to reactor length L, $U_o L D_{ax}^{-1} \epsilon^{-1}$
Pe_{pore}	Peclet number based on mean pore diameter d_p, $\tau U_o d_p \epsilon^{-1} D_{ax}^{-1}$
Pe_1	Peclet number related to a reactor length L equal to 1 m, $U_o D_{ax}^{-1} \epsilon^{-1}$
Re_o	superficial Reynolds number, $\rho U_o D \mu^{-1}$
Re_{pore}	Reynolds number based on mean pore diameter d_p, $\rho U_o \tau d_p \epsilon^{-1} \mu^{-1}$
U	mean velocity in pores, $U_o \tau \epsilon^{-1}$ (m s^{-1})
U_o	superficial velocity (m s^{-1})
z	axial position (m)

Greek letters

α	coefficient in eqn. (2) (m)
ϵ	bed void fraction of porous medium
μ	dynamic viscosity of electrolyte (Pa s)
ρ	electrolyte density (kg m^{-3})
τ	tortuosity of porous medium